By constructing a model of X and Y zeolites we find that on either of these sites a methanol molecule will have three nearest neighbors at about 0.4 nm if the methanolic oxygen is located ~0.25 nm above the square or hexagonal faces with the molecular dipole pointing toward the center of the face. This is in good agreement with our experimental results and 0.25 nm is a reasonable distance for coordination of the oxygen to a cation in the square or hexagonal face. This model indicates a cation-to-radical site distance of 0.38–0.40 nm. Spin–echo studies of hydroxymethyl radicals in CsX, CsY, LiX, and LiY zeolites have also been made.[20] In these studies the modulation from the cation could be clearly seen and the analysis indicates a cation-to-radical site distance of 0.40–0.45 nm. This again is in agreement with our model.

For a hydrogen bond between the hydroxyl proton and a lattice oxygen to be not too weak, the molecular dipole has to be tilted away from the threefold axis of a hexagonal face or the fourfold axis of a square face. A tilt of 5–10° seems to be reasonable as shown in Figure 7C and such an arrangement explains the 0.47-nm distance obtained from the analysis of deuterium modulation in CH_3OD adsorbed X zeolites. Modulation is not seen from the α-deuterons on the radical itself because the hyperfine coupling is so large that conditions for producing modulation are not met.[7]

In our earlier paper on hydroxymethyl radicals in X, Y, and A zeolites, the aluminum modulations were interpreted on the basis of the Al/Si ratio in these zeolites.[10] Accordingly, a radical situated above a square or hexagonal face of the α-cage in line with a lattice Al(Si) ion was shown to interact with 0.4, 0.3, or 0.5 Al ions as determined by the factor $n_{Al}/(n_{Al} + n_{Si})$ in the lattice of X, Y, and A zeolites. However, unless the radical is flipping between the Al and Si ion sites, one radical would interact with Al and another with Si and their contributions to the net echo decay would be additive.[21] Hence the modulation amplitude should be

$$V_{mod} = \frac{n_{Si}}{n_{Si} + n_{Al}} V_1 + \frac{n_{Al}}{n_{Si} + n_{Al}} V_2$$

and not $(V)^{n_{Al}/(n_{Al}+n_{Si})}$ as given earlier.[10] However, the number of aluminum ions interacting with the radical would still be governed by Al/Si ratio. This is because the first term would only contribute to the decay and not to the modulation since the Si nuclei have zero nuclear spin.

Conclusions

From the analysis of modulations observed in the echo decay curves of hydroxymethyl radicals in A, X, and Y zeolites information about the location and relative orientation of methanol molecules in these zeolites is obtained. In A zeolites the hydroxymethyl radical is located in the α-cage above a hexagonal window with the molecular dipole oriented along the threefold axis. It interacts with three other equivalent closest methanol molecules in the α-cage with their methyl groups at 0.38 nm from the radical site. In X and Y zeolites the radical is also located in the α-cage above a hexagonal window or square face and interacts with three equivalent closest methanol molecules at 0.40–0.42 nm. A model consistent with these numbers and distances is proposed.

Acknowledgment. This research was supported by the Department of Energy and the National Science Foundation. We thank Dr. R. Janakiraman for helpful discussions.

(21) Tsvetkov, Yu. D.; Dikanov, S. A., 1979, private communication.

Mechanism of Oxidation of an Amine Coordinated to Ruthenium

Michael J. Ridd and F. Richard Keene*

Contribution from the Department of Chemistry and Biochemistry, James Cook University of North Queensland, Townsville, Queensland 4811, Australia. *Received November 17, 1980*

Abstract: The mechanism of the oxidative dehydrogenation of $[Ru(bpy)_2ampy]^{2+}$ (bpy = 2,2′-bipyridine; ampy = 2-(aminomethyl)pyridine) to the corresponding imine complex has been studied in aqueous media by using stopped-flow methods in association with chemical oxidation by Ce(IV), flash photolysis techniques, and electrochemical methods. Solutions to the rate laws for several possible mechanisms were obtained numerically and the spectrophotometric responses matched with the theoretical solutions by use of a nonlinear optimization program. The data were found to be consistent with a mechanism involving a Ru(IV) species in which the ampy ligand is deprotonated, and this intermediate subsequently undergoes a two-electron transfer (accompanied by deprotonation) to give the imine product. The various rate constants for the individual steps of the mechanistic scheme were consistent with values for electron-transfer reactions and proton equilibria in similar metal complex systems.

The oxidative dehydrogenation of amines to imines or nitriles is known to be catalyzed by their coordination to metal centers. Initial studies of the oxidation of macrocyclic amines were made by Curtis[1] and Busch,[2] and recent studies[3,4] have confirmed the earlier assertion[2] that such reactions involved initial oxidation of the metal center followed by an intramolecular redox process in which the ligand is oxidized and the metal reduced.

The analogous oxidation of coordinated ethylenediamine to the corresponding α,α'-diimine has also been reported,[5-7] and Meyer et al.[8] and Ford et al.[9] have studied the oxidation of a range of bidentate amines coordinated to ruthenium. The oxidative de-

(1) Curtis, N. F. *Coord. Chem. Rev.* **1968**, *3*, 3–47 and references therein.
(2) Goedken, V. L.; Busch, D. H. *J. Am. Chem. Soc.* **1972**, *94*, 7355–7363. Hipp, C. J.; Lindoy, L. F.; Busch, D. H. *Inorg. Chem.* **1972**, *11*, 1988–1994.
(3) Maruthamuthu, P.; Patterson, L. K.; Ferraudi, G. *Inorg. Chem.* **1978**, *17*, 3157–3163.
(4) Jaacobi, M.; Meyerstein, D.; Lilie, J. *Inorg. Chem.* **1979**, *18*, 429–433.
(5) Beattie, J. K.; Elsbernd, H. *J. Chem. Soc. A* **1970**, 2598–2600.
(6) Lane, B. C.; Lester, S. E., Basolo, F. *Chem. Commun.* **1971**, 1618–1619.
(7) Goedken, V. L. *J. Chem. Soc., Chem. Commun.* **1972**, 207–208.
(8) Brown, G. M.; Weaver, T. R.; Keene, F. R.; Meyer, T. J. *Inorg. Chem.* **1976**, *15*, 190–196.
(9) Alvarez, V. E.; Allen, R. J.; Matsubara, T.; Ford, P. C. *J. Am. Chem. Soc.* **1974**, *96*, 7686–7692.

0002-7863/81/1503-5733$01.25/0 © 1981 American Chemical Society

hydrogenation of monodentate primary amines proceeds further and produces the corresponding nitriles.[10-12] The oxidations of coordinated alcohols to the corresponding aldehyde or ketone have also been reported.[13,14]

In all these studies of oxidative dehydrogenation reactions of coordinated ligands, limited detailed mechanistic information is available, except that the oxidation of the metal center appears to precede ligand reaction. Recent pulse radiolysis studies of nickel macrocyclic complexes[3] have been interpreted to indicate that following the initial Ni(II) → Ni(III) oxidation, a series of reactions occurs which involve a Ni(II)–radical species: the overall process is then completed by the one-electron oxidation of this radical species, yielding the dehydrogenated product. An alternative mechanism for the oxidation of an alcohol coordinated to a ruthenium center has been proposed by Tovrog et al.[14] which involves initial oxidation of the metal center from ruthenium(II) to ruthenium(III), followed by a disproportionation to form a Ru(IV) species which undergoes a two-electron reduction with concomitant two-electron oxidation of the ligand.

While it may be unlikely that the mechanism of ligand dehydrogenation is uniform throughout the range of metals and ligands for which such reactions have been observed, the general phenomenon is of considerable interest as the reactions are quantitative, in contrast to the oxidation of uncoordinated amines and alcohols. We have undertaken a detailed investigation of the oxidation of a number of amine and alcohol substrates coordinated to a variety of metal ions: we now report mechanistic studies of the oxidation of 2-(aminomethyl)pyridine (ampy) coordinated to ruthenium, using techniques of chemical oxidation, electrochemical oxidation, and flash photolysis. This particular system was chosen since the oxidation reaction (1) is well characterized[8] and yields

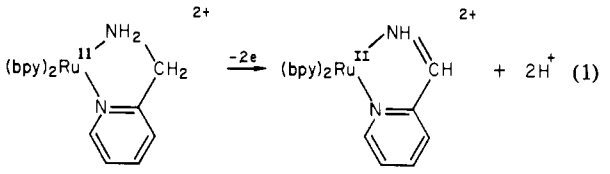

(1)

a stable product (a conjugated α,α'-diimine): furthermore, since it involves two electrons only it represents perhaps the simplest amine dehydrogenation reaction.

Experimental Section

Measurements. Electronic spectra were recorded by using a Cary 118C or Varian 634S spectrophotometer and emission spectra by using a Perkin-Elmer 3000 fluorescence spectrometer. The cell compartments were unthermostated.

All electrochemical measurements were made vs. the saturated sodium chloride calomel electrode (SSCE) at 25 ± 2 °C and are uncorrected for junction potentials. Potential control was obtained by using a Utah Electronics 0152 potentiostat and in conjunction with a Utah Electronics 0151 sweep generator for the voltammetric experiments. Slow scan cyclic voltammograms and single-sweep voltammograms were recorded by using a Houston Omnigraphic 2000 X-Y recorder. Fast scan cyclic voltammograms were obtained photographically from the trace on a Tektronix DM64 storage oscilloscope. Coulometry was performed by using a Fisher controlled potential electroanalyzer, Model 9-264-100, using platinum gauze electrodes. The charge passed was calculated by measuring the area under the i vs. t curve after the current had dropped to 1% of its initial value.

The details of the equipment used in the double-potential step experiments have been described elsewhere.[15] The pulse generator was built in the department.[16] Timing pulses were produced by a Digitimer D-4030 quartz-locked timer: current–time or charge–time responses were stored by a Biomation 805 waveform recorder, from which the output was displayed by using a Houston Omnigraphic 2000 X-Y recorder.

Elemental analyses were carried out by the Australian Microanalytical Service, CSIRO, Melbourne.

Materials. Tetra-*n*-butylammonium hexafluorophosphate (TBAH), used as an electrolyte for the electrochemical measurements, was prepared and purified by standard techniques.[17] The ligands 2,2′-bipyridine (Sigma), 2,2′:6′,2″-terpyridine (Sigma), and 2-(aminomethyl)pyridine (Aldrich) were used without purification. Propylene carbonate (Aldrich) was distilled immediately before use (90–92 °C (3.5 mmHg)) and stored over 4A molecular sieves. The complex $[Ru(bpy)_2Cl_2]\cdot 2H_2O$ was prepared as described previously.[18] Cerium ammonium sulfate (Fluka; puriss) was determined spectrophotometrically in 2 M H_2SO_4 against a standardized Ce(IV) solution and found to be $(NH_4)_4Ce(SO_4)_4\cdot 2H_2O$. All other chemicals were A.R. grade and were used without further purification.

Preparation of Complexes. (2-(Aminomethyl)pyridine)bis(2,2′-bipyridine)ruthenium(II) Perchlorate, $[Ru(bpy)_2(ampy)](ClO_4)_2$, was prepared in 72% yield by literature methods.[8] The complex was further purified by the following chromatographic procedure. An aqueous solution of the complex was sorbed on to a column of SP-Sephadex C25 cation exchanger and eluted with 1 M KNO_3. Two bands were observed, and the first (more intense) band was collected and evaporated to dryness. The residue was extracted with ethanol and the extract filtered and evaporated to dryness yielding the nitrate salt of the complex. The solid was dissolved in a minimum volume of water and the solution filtered and heated to 80–90 °C on a steam bath: addition of solid $NaClO_4$ and cooling led to crystallization of the perchlorate salt with 80% recovery. The visible spectrum in water showed $\epsilon_{471}^{max} = 10\,200$ and $\epsilon_{340}^{max} = 10\,800$, and cyclic voltammetry (propylene carbonate/0.2 M TBAH; glassy carbon electrode) gave $E_{1/2} = 1.16$ V vs. SSCE. Anal. Calcd for $RuC_{26}H_{24}N_6O_8Cl_2$: C, 33.3; H, 3.36; N, 11.7. Found: C, 33.2; H, 3.27; N, 11.4. The complex could also be obtained as the hexafluorophosphate salt by precipitation with NH_4PF_6.

(2-(Iminomethyl)pyridine)bis(2,2′-bipyridine)ruthenium(II) hexafluorophosphate, $[Ru(bpy)_2(impy)](PF_6)_2$, was prepared by literature methods,[8] and chromatographically purified as described for the corresponding ampy complex. The visible spectrum in water gave $\epsilon_{470}^{max} = 13\,600$ and cyclic voltammetry indicated $E_{1/2} = 1.33$ V vs. SSCE (propylene carbonate/0.2 M TBAH; glassy carbon electrode). Anal. Calcd for $RuC_{26}H_{22}N_6P_2F_{12}$: C, 38.6; H, 2.74; N, 10.4. Found: C, 38.8; H, 2.81; N, 10.4.

Trichloro(terpyridine)ruthenium(III), $[Ru(tpy)Cl_3]$, and (Bipyridine)chloro(terpyridine)ruthenium(II) hexafluorophosphate, $[Ru(tpy)(bpy)Cl]PF_6$, were prepared and purified by using methods supplied by Meyer et al.[19]

Aquo(bipyridine)(terpyridine)ruthenium(II) Perchlorate, $[Ru(tpy)(bpy)OH_2](ClO_4)_2$. $[Ru(tpy)(bpy)Cl]PF_6$ (0.39 g, 0.58 mmol) was suspended in water (20 mL) and $AgNO_3$ (0.39 g, 2.3 mmol) added. The mixture was protected from the light, stirred for 1 h, and then filtered. When solid $NaClO_4$ was added to the filtrate, the product crystallized (0.19 g, 51%). The visible spectrum in water gave $\epsilon_{477}^{max} = 8700$ and from cyclic voltammetry $E_{1/2} = 1.10$ V vs. SSCE (propylene carbonate/0.2 M TBAH; glassy carbon electrode).

Ammine(bipyridine)(terpyridine)ruthenium(II) Hexafluorophosphate, $[Ru(tpy)(bpy)NH_3](PF_6)_2$. $[Ru(tpy)(bpy)OH_2](ClO_4)_2$ (100 mg) was dissolved in water (10 mL) and ammonia bubbled through the solution until saturation. The solution was sealed in

(10) McWhinnie, W. R.; Miller, J. D.; Watts, J. B.; Wadden, D. Y. *Inorg. Chim. Acta* **1973**, *7*, 461–466.
(11) Diamond, S. E.; Tom, G. M.; Taube, H. *J. Am. Chem. Soc.* **1975**, *97*, 2661–2664.
(12) Keene, F. R.; Salmon, D. J.; Meyer, T. J. *J. Am. Chem. Soc.* **1976**, *98*, 1884–1889.
(13) Reichgott, D. W.; Rose, N. J. *J. Am. Chem. Soc.* **1977**, *99*, 1813–1818.
(14) Tovrog, B. S.; Diamond, S. E.; Taube, H. *J. Am. Chem. Soc.* **1979**, *101*, 5067–5069.
(15) Buess, P. Ph.D. Thesis, Université Libre de Bruxelles, 1970.
(16) Based on plans provided by Professor L. Gierst (Université Libre de Bruxelles).
(17) Ferguson, J. A.; Meyer, T. J. *Inorg. Chem.* **1972**, *11*, 631–636.
(18) Sullivan, B. P.; Salmon, D. J.; Meyer, T. J. *Inorg. Chem.* **1978**, *17*, 3334–3341.
(19) Meyer, T. J., personal communication.

a glass tube and heated at 100 °C for 2 h. After the solution was cooled, NH_4PF_6 (0.5 g) was added and the complex extracted with dichloromethane. The organic phase was dried with sodium sulfate and evaporated to dryness (75 mg, 67%). The complex was recrystallized from hot methanol with 80% recovery. Visible spectrum ϵ_{482}^{max} = 10 000 (water) and from cyclic voltammetry, $E_{1/2}$ = 1.02 V vs. SSCE (propylene carbonate/0.2 M TBAH; glassy carbon electrode). Anal. Calcd for $RuC_{25}H_{22}N_6P_2F_{12}$: C, 37.6; H, 2.78; N, 10.5. Found: C, 37.3; H, 2.92; N, 10.4.

Chemical Oxidations. Spectrophotometric Titrations. Aliquots (10 mL) of a 1.07×10^{-4} M solution of $[Ru(tpy)(bpy)NH_3]^{2+}$ in 1 M H_2SO_4 were added to each of five 25 mL volumetric flasks. Aliquots of a 2.66×10^{-4} M solution of Ce(IV) in 1 M H_2SO_4 were added so that the Ce/Ru ratio was varied from 0 to 2, the flasks made up to the required volume with 1 M H_2SO_4, and the visible/UV spectra measured by using a Cary 118C spectrophotometer.

For $Ru(bpy)_2ampy^{2+}$, a similar procedure was followed by using 50-mL flasks with 20-mL aliquots of 7.39×10^{-5} M $Ru(bpy)_2ampy^{2+}$ solution and 1.48×10^{-4} M Ce(IV). The Ce/Ru ratio was varied from 0 to 2.5.

Kinetic Apparatus. An Aminco-Morrow stopped-flow apparatus at the Australian Atomic Energy Commission, Lucas Heights, was used to monitor the reactions: the apparatus and the computerized data acquisition system are described elsewhere.[20] Analysis of the kinetic data was undertaken on the IBM 370 computer at A.A.E.C. or on the PDP-10 system at James Cook University of North Queensland.

Oxidation of $[Ru(tpy)(bpy)NH_3]^{2+}$ by Ce(IV). The kinetics were followed under second-order conditions at λ = 482 nm. The complex and Ce(IV) solutions in H_2SO_4 solution of the appropriate concentration were thermostated to 20 °C, as was the syringe block and mixing chamber of the stopped-flow apparatus. For the oxidation reaction

$$Ce(IV) + Ru^{II}(tpy)(bpy)NH_3^{2+} \xrightarrow{k} Ce(III) + Ru^{III}(tpy)(bpy)NH_3^{3+}$$

only $Ru(tpy)(bpy)NH_3^{2+}$ absorbs at λ = 482 nm. Consequently, if A_0 and B_0 are the initial concentrations of the respective reactants, D is the absorbance at time t, and ϵ is the molar extinction coefficient of the Ru(II) species, it can easily be shown that for a second-order process

$$\frac{1}{B_0 - A_0} \log \left\{ \frac{D/\epsilon}{(B_0 - A_0 + D/\epsilon} \right\} = kt + c$$

Oxidation of $[Ru(bpy)_2ampy]^{2+}$ by Ce(IV). The experimental conditions were as described for the oxidation of $[Ru(tpy)(bpy)NH_3]^{2+}$, with the reaction being monitored at λ = 471 nm.

The analysis of the stopped flow data for (2-(aminomethyl)pyridine)bis(2,2′-bipyridine)ruthenium(II), $Ru(bpy)_2ampy^{2+}$, is considerably more complicated than that for $[Ru(tpy)(bpy)NH_3]^{2+}$, since several steps follow the Ru^{2+}/Ru^{3+} oxidation in the overall reaction mechanism. It was not possible to obtain analytical solutions to the rate law differential equations for the reaction mechanisms considered. The differential equations were numerically solved, and the values of the rate constants resulting in the best fit between experimental and calculated responses were obtained by using nonlinear programming techniques. For a description of the numerical analysis and the nonlinear optimization techniques used, see the Appendix.

Flash Photolysis Studies. The laser photolysis and flash photolysis facilities at the University of Adelaide were used for these studies; a description of this equipment and of the data acquisition system is given elsewhere.[21]

Luminescence lifetime measurements and quenching rate measurements (by $Fe(OH_2)_6^{3+}$) were carred out by laser photolysis in 1 M H_2SO_4 and 1 M $HClO_4$, using a complex concentration of 1.00×10^{-5} M. All solutions were deaerated (using N_2) before use and thermostated at 25 °C. All runs were monitored at 629 nm.

For the flash photolysis studies of the ligand oxidation reaction, the complex concentration was maintained at 1.00×10^{-5} M, $[Fe^{3+}]$ was maintained at 2.0×10^{-3} M, and $[HClO_4]$ (or $[H_2SO_4]$) varied from 1.0 to 0.01 M. Ionic strength was maintained at μ = 1 by using $NaClO_4$ or $NaHSO_4$, respectively. Each solution was deaerated before use (using N_2). Measurements were made in cylindrical 10-cm cells and conducted at room temperature (24.0 ± 0.5 °C). Each solution was used for one flash experiment only, and 3–4 determinations were conducted for each set of conditions. At an acid concentration of 1 M, a set of measurements was made in which the intensity of the flash was varied. All flash photolysis experiments were monitored at 436 nm.

Results and Discussion

The oxidation of 2-(aminomethyl)pyridine coordinated to ruthenium is given by the stoichiometric eq 1. The reaction has been reported previously[8] to be rapid and quantitative in acetonitrile solution, whether promoted chemically (by Ce(IV)) or electrochemically. Since electron exchange involving metal ions is often rapid[22] and electron-transfer processes between metal ions and electrode surfaces are likely to be rapid, it is assumed that the initial step in a reaction such as above would be a Ru(II) → Ru(III) oxidation

$$Ru^{II}(bpy)_2(ampy)^{2+} \xrightarrow{-e} Ru^{III}(bpy)_2(ampy)^{3+} \qquad (2)$$

The elucidation of the mechanism of the subsequent ligand oxidation requires a rapid method for promotion of the prior metal oxidation: we now report kinetic studies of such reactions by using flash photolysis techniques, electrochemical studies, and chemical oxidation by Ce(IV) in association with stopped-flow methods.

The oxidative dehydrogenation of the ligand is required to be a two-electron process, which may proceed via two successive one-electron transfers or by a two-electron transfer from metal to ligand. The former possibility has been proposed in the mechanistic studies of the oxidation of nickel(II) macrocycles[3] by using pulse radiolysis techniques. These data were interpreted to indicate that ligand dehydrogenation occurred by initial oxidation of the metal (Ni(II) → Ni(III)) followed by a deprotonation at the coordinated amine nitrogen group: the resultant Ni(III)–conjugate base species then underwent an intramolecular one-electron transfer to give a Ni(II)–radical species. A subsequent one-electron oxidation of the ligand radical results in the loss of a further proton from the α-carbon atom.

A second mechanistic proposal has been suggested for the ruthenium-promoted oxidation of 2-(1′-hydroxyethyl)pyridine[14] and involves a Ru(IV) intermediate formed by disproportionation of the Ru(III) species. Such disproportionation processes have been reported previously for $Ru(NH_3)_5py^{3+}$.[23] The Ru(IV) intermediate subsequently undergoes an intramolecular redox process resulting in a two-electron reduction of the metal and oxidative dehydrogenation of the ligand.

Chemical Oxidation Studies. The Ru(III)/Ru(II) couple for $[Ru(bpy)_2ampy]^{n+}$ occurs at a sufficiently anodic potential ($E_{1/2}$ = 1.12 V in acetonitrile; $E_{1/2}$ = 1.16 V in propylene carbonate; $E_{p,a}$ = 0.76 V in 1 M H_2SO_4: all potentials relative to SSCE) that there are a limited number of appropriate chemical oxidants. Cerium(IV) was used for the present studies, and all runs were carried out at constant sulfuric acid concentration (1 M) to avoid problems with anion dependencies and hydrolysis equilibria.[24,25]

In mechanistic schemes for the ligand oxidation of $[Ru(bpy)_2ampy]^{2+}$ based on the two proposals outlined above, the

(20) Ekstrom, A. *Inorg. Chem.* **1973**, *12*, 2455–2460.
(21) Thornton, A. T.; Laurence, G. S. *Radiat. Phys. Chem.* **1978**, *11*, 311–319.
(22) Wilkins, R. G. "The Study of Kinetics and Mechanism of Reactions of Transition Metal Complexes"; Allyn and Bacon: Boston, 1976.
(23) Rudd, De F. P.; Taube, H. *Inorg. Chem.* **1971**, *10*, 1543–1544.
(24) Michaille, P.; Kikindai, T. *J. Inorg. Nucl. Chem.* **1977**, *39*, 859–864.
(25) Benson, D. "Mechanism of Oxidation by Metal Ions"; Elsevier: New York, 1976.

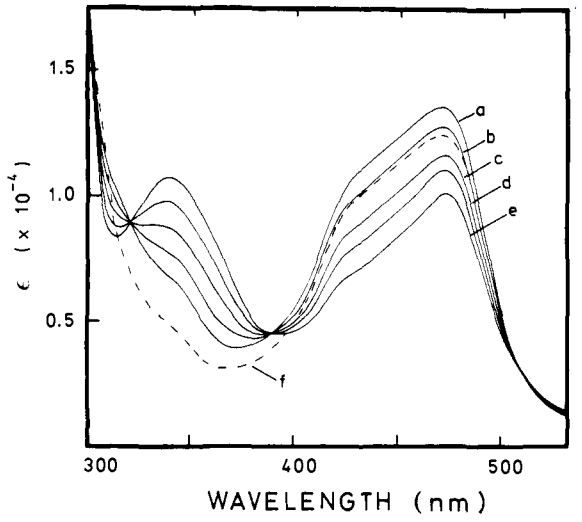

Figure 1. Spectrophotometric titration of $Ru(bpy)_2ampy^{2+}$ with Ce(IV) in 1 M H_2SO_4: Ce/Ru ratio (a) 0, (b) 0.5:1, (c) 1:1, (d) 1.5:1, (e) 2:1, (f) 2.5:1.

initial step is given by eq 2. In order to gain some insight into the rate of this reaction, we studied the oxidation of ammine(bipyridine)(terpyridine)ruthenium(II), $[Ru(tpy)(bpy)NH_3]^{2+}$. Since both $[Ru(tpy)(bpy)NH_3]^{2+}$ and $[Ru(bpy)_2ampy]^{2+}$ have five pyridine nitrogens and one amine nitrogen coordinated to a ruthenium(II) metal center, the rates of oxidation of the ruthenium(II) center to the corresponding 3+ state should be similar. The ligands in $[Ru(tpy)(bpy)NH_3]^{2+}$ are not susceptible to oxidation under the conditions of the experiment, so that the reaction may not proceed further than

$$Ce(IV) + Ru(tpy)(bpy)NH_3^{2+} \xrightarrow{k} Ce(III) + Ru(tpy)(bpy)NH_3^{3+} \quad (3)$$

for which the calculation of the rate constant is quite simple: by comparison, for $[Ru(bpy)_2ampy]^{2+}$ further ligand oxidations make the kinetic solutions complicated.

A spectrophotometric titration of $[Ru(tpy)(bpy)NH_3]^{2+}$ with Ce(IV) in 1 M H_2SO_4 shows a clean one-electron oxidation of the complex to Ru(III), with an isosbestic point at $\lambda = 354$ nm up to a Ce/Ru ratio of 1:1. In the kinetic study of reaction 3, stopped-flow measurements at $\lambda = 482$ nm gave data which showed second-order behavior and indicated $k = 6.1\ (\pm 0.2) \times 10^5\ M^{-1}\ s^{-1}$ at 20 °C.

A spectrophotometric titration of $Ru(bpy)_2ampy^{2+}$ with Ce(IV) in 1 M H_2SO_4 shows a clean two-electron oxidation of the complex to $Ru(bpy)_2impy^{2+}$.

$$2Ce(IV) + Ru(bpy)_2ampy^{2+} \rightarrow 2Ce(III) + Ru(bpy)_2impy^{2+} + 2H^+ \quad (4)$$

Figure 1 shows isosbestic points (at $\lambda = 512$, 389, and 322 nm) up to a Ce/Ru ratio of 2:1. There are further isosbestic points (at $\lambda = 239$, 251, and 286 nm). Addition of greater than 2 equiv of cerium(IV) resulted in the loss of the isosbestic points, indicating a further reaction, probably

$$Ru^{II}(bpy)_2impy^{2+} + Ce(IV) \rightarrow Ru^{III}(bpy)_2impy^{3+} + Ce(III) \quad (5)$$

A similar experiment[8] in a nonaqueous solvent (acetonitrile) revealed similar behavior.

The kinetics of the above reaction were followed in 1 M H_2SO_4 by using stopped-flow techniques, and a typical response is shown in Figure 2. An attempt was made to fit the observed responses to a number of mechanistic schemes based on the intermediacy of either a Ru(II)-free radical species or a Ru(IV) species formed by disproportionation. The programs (see Appendix) produced a numerical solution to the set of differential equations appropriate to each scheme, and a nonlinear optimization procedure then varied the rate constants for each scheme to minimize the difference between the calculated and observed transmittance–time responses. An excellent correlation was found for the mechanistic scheme shown in eq 6–9.

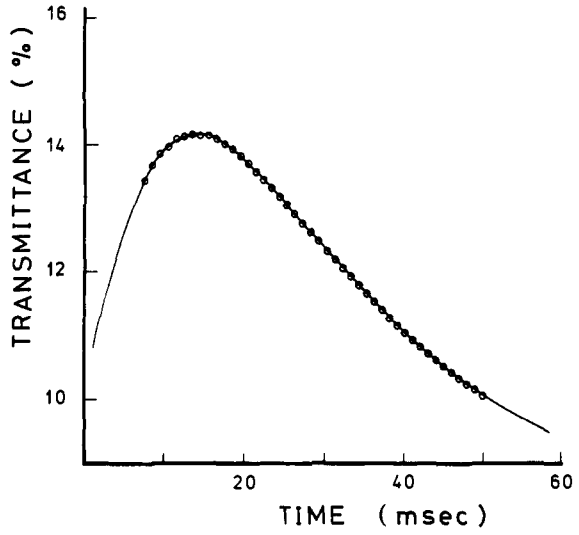

Figure 2. Calculated transmittance–time curve (—) for the oxidation of $Ru(bpy)_2ampy^{2+}$ with Ce(IV) and the observed response (O) ($[H_2SO_4] = 1$ M; $[Ru(bpy)_2ampy^{2+}] = 1.04 \times 10^{-4}$ M; $[Ce(IV)] = 8.8 \times 10^{-5}$ M).

$$(bpy)_2Ru^{II}ampy^{2+} \underset{-e}{\xrightarrow{k_1}} (bpy)_2Ru^{III}ampy^{3+} \quad (6)$$

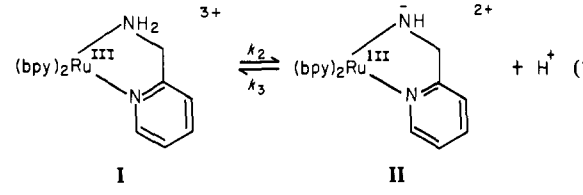

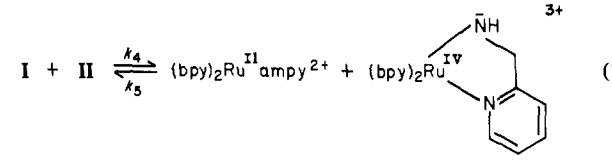

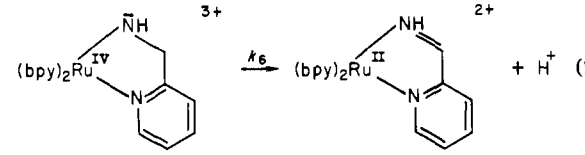

Figure 2 shows the calculated transmittance–time response based on the above mechanism and the conditions of the experimental curve shown: the calculated curves are quite sensitive to small changes in the values of the rate constants.

Much less satisfactory fits were obtained for any scheme based on the free radical proposal.

Two assumptions are made in the formulation of the differential equations and in the simulation of the absorbance–time responses. First, the oxidation of the metal center is assumed to be the initial step in the reaction. Second, it has been assumed that any Ru(III) species are optically transparent in the visible region of the spectrum: the strong visible absorption of (bipyridine)ruthenium(II) complexes is due to $d\pi[Ru(II)]-\pi^*(bpy)$ metal-to-ligand charge-transfer (MLCT) transitions,[26] and on oxidation of the metal to Ru(III), this absorption would be expected to be lost.[27] For the related complex ammine(bipyridine)(terpyridine)ruthenium(III), $[Ru(tpy)(bpy)NH_3]^{3+}$, $\epsilon < 300\ M^{-1}\ cm^{-1}$ for wavelengths greater than 425 nm. For a Ru(IV) species, however,

(26) Bryant, G. M.; Fergusson, J. E.; Powell, H. K. J. *Aust. J. Chem.* **1971**, *24*, 257–273.
(27) Bryant, G. M.; Fergusson, J. E. *Aust. J. Chem.* **1971**, *24*, 275–286.

Table I. Calculated Rate Constants for the Scheme Given in Eq 6–9 Using Data from Various Techniques

reaction[a]	Ce(IV) studies in 1 M H_2SO_4[b]	flash photolysis in 1 M H_2SO_4[c,d]	flash photolysis in $HClO_4$[c,e]
(i) k_1, M^{-1} s^{-1}	5×10^5		
k_2, s^{-1}	4×10^6	4×10^6	5×10^6
k_3, M^{-1} s^{-1}	3×10^9	2×10^9	1×10^9
k_4, M^{-1} s^{-1}	6×10^8	9×10^8	1×10^9
k_5, M^{-1} s^{-1}	4×10^6	5×10^6	5×10^6
k_6, s^{-1}	102	90	93
ϵ, M^{-1} cm^{-1}	300[f]	1100[g]	1250[g]
(ii) k_1, M^{-1} s^{-1}	5×10^5		
k_2, s^{-1}	5×10^9	3×10^9	5×10^9
k_3, M^{-1} s^{-1}	2×10^{10}	1×10^{10}	1×10^{10}
k_4, M^{-1} s^{-1}	8×10^8	1×10^9	1×10^9
k_5, M^{-1} s^{-1}	4×10^8	4×10^8	4×10^8
k_6, s^{-1}	760	910	950
ϵ, M^{-1} cm^{-1}	400[f]	950[g]	900[g]

[a] (i) and (ii) correspond to different numerical solutions to minimization. [b] 20 °C. [c] 24 °C. [d] Averaged values for $[H_2SO_4] = 1.00$ M. [e] Average values over $[HClO_4] = 0.01$–1.00 M. [f] $\lambda = 471$ nm. [g] $\lambda = 436$ nm.

absorption in this region may be somewhat larger. Comparison of the spectra of aquo(bipyridine)(terpyridine)ruthenium(II) and its two-electron oxidation product, identified by Meyer et al.[28] as oxo(bipyridine)(terpyridine)ruthenium(IV), shows the extinction coefficients at $\lambda = 471$ nm and $\lambda = 436$ nm (the wavelengths at which the present reactions were studied) to be 550 and 1150, respectively. Since ϵ for the $(bpy)_2Ru^{IV}(ampy\text{-}H)^{3+}$ species was not known, ϵ was included as a variable along with the rate constants k_1–k_6 for the numerical analysis of the mechanism given in the scheme. The only ruthenium(II) species involved are $[Ru(bpy)_2ampy]^{2+}$ and $[Ru(bpy)_2impy]^{2+}$, for which the molar extinction coefficients are known.

It was found that there were two solutions to the minimization procedure, and the values of the rate constants and extinction coefficient for each numerical solution are given in Table I. A discussion is given subsequently with the flash photolysis results.

The limitations of the use of chemical oxidation of $Ru(bpy)_2ampy^{2+}$ by Ce(IV) in a kinetic study lie in the inability to obtain information at varying acid concentrations, due to the complicated hydrolysis behavior of Ce(IV) under different pH conditions. Such data can be obtained by using flash photolysis techniques, as described subsequently.

Electrochemical Studies. Electrochemical study of the oxidation of coordinated ligands is attractive because the initial oxidation of the metal center at the electrode surface can be made to be diffusion controlled. A constraint on obtaining quantitative data from the electrochemical studies is that the theory for the analysis of relatively complex chemical reaction schemes associated with the electrode process (such as occur in this study) has not been fully developed. For this reason, much of the electrochemical data is somewhat qualitative in nature.

Previous preliminary studies on this system[8] revealed that in acetonitrile and acidic aqueous solution, a two-electron oxidation occurred on coulometry to give the imine species quantitatively. Cyclic voltammetric studies revealed that the complex had an irreversible oxidation in aqueous solution for any scan rate and an irreversible couple at slow scan rate in acetonitrile, although some evidence was obtained for the Ru(III) → Ru(II) reverse wave at high scan rates.[8]

In the course of the present study, we have reexamined the electrochemistry of this system in propylene carbonate and aqueous sulfuric acid media. The cyclic voltammetry in propylene carbonate and 1 M H_2SO_4 at low scan rates is irreversible with the reduction peak for the couple not being observed. Another reversible couple is observed at a potential anodic of the $Ru(bpy)_2ampy^{2+}$ system ($E_{1/2} = 1.33$ V vs. SSCE for propylene carbonate, $E_{1/2} = 0.97$ V vs. SSCE for 1 M H_2SO_4) corresponding to the dehydrogenated species $Ru(bpy)_2impy^{3+/2+}$ and showing that the ligand oxidation is completed in the time scale of the scan. The slow sweep cyclic voltammogram of $Ru(bpy)_2(ampy)^{3+/2+}$ in propylene carbonate is given in Figure 3.

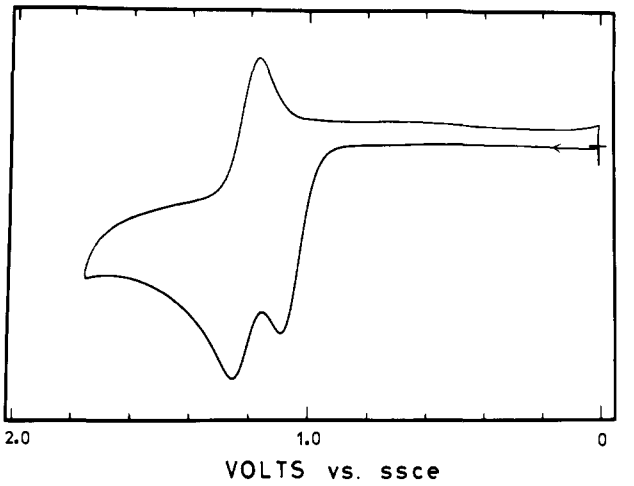

Figure 3. Slow sweep rate (50 mV/s) cyclic voltammogram of 1.07 mM $Ru(bpy)_2ampy^{2+}$ (propylene carbonate/0.2 M TBAH; glassy carbon electrode).

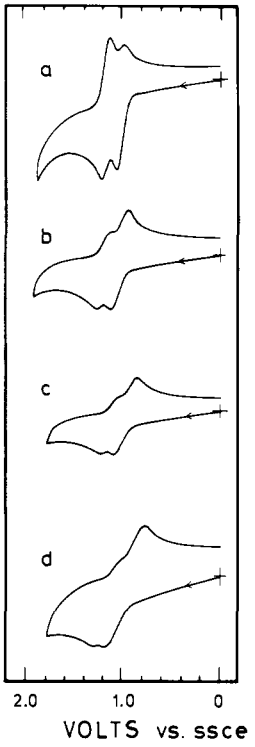

Figure 4. Effect of increasing sweep rate on the cyclic voltammetry of $Ru(bpy)_2ampy^{2+}$ in propylene carbonate/0.2 M TBAH (glassy carbon electrode): (a) sweep rate = 100 mV/s; (b) sweep rate = 1 V/s; (c) sweep rate = 5 V/s; (d) sweep rate = 10 V/s.

Figure 4 shows the effect of increasing the sweep rate of the cyclic voltammetry of $Ru(bpy)_2ampy^{2+}$ in propylene carbonate. As the sweep rate is increased, the reverse peak of the $Ru(bpy)_2ampy^{3+/2+}$ couple is observed and increases in magnitude as the sweep rate increases. Similar behavior may be observed in 5 M H_2SO_4. In 1 M H_2SO_4, it was not possible to observe the reverse peak of the $Ru(bpy)_2ampy^{3+/2+}$ couple at scan rates of up to 100 V/s: an inverse proton dependence of the rate of ligand oxidation would be expected for either of the mechanistic proposals.

Single potential step chronocoulometry studies in propylene carbonate and aqueous acidic solutions using a glassy carbon

(28) Moyer, B. A.; Meyer, T. J. *J. Am. Chem. Soc.* **1978**, *100*, 3601–3603.

working electrode reveal linear Q vs. $t^{1/2}$ plots with zero intercept after correction for the double-layer charging current. Such results indicate that there are no chemical reactions prior to the initial electrode promoted Ru(II) → Ru(III) oxidation, which is diffusion controlled, and that there is no adsorption of reactant on to the electrode surface. Hence, mass-transfer electrochemical techniques should be applicable to the present system.

It was hoped that during the course of this work, the techniques of double potential step chronocoulometry and chronoamperometry might be used in the elucidation of the mechanistic path of these oxidation reactions. Reilley et al.[29] have published calculations of electrochemical responses by using these techniques for 22 different cases of chemical reactions associated with electrochemical steps. At present, quantitative analysis of the responses from double potential step chronocoulometry or chronoamperometry is not possible for the $Ru(bpy)_2ampy^{2+}$ system because of deficiencies in the available mathematical treatment of a series of interrelated chemical and electrochemical reactions of this complexity. Work on developing the analysis of such responses for kinetic studies of coordinated ligand redox processes is currently in progress.

Preliminary double potential step chronoamperometric studies are consistent with a scheme involving a disproportionation following the initial oxidation process. Marcoux[30] has described a technique, called potential dependent chronoamperometry, in which the potential is not necessarily stepped into the region of diffusion control. Variation of the applied potential permits systematic variation of the concentration ratios within the diffusion layers adjacent to an electrode. Consequently, by variation of the upper limiting potential to a small increment (~60 mV) either side of the redox couple, Marcoux[30] found that I vs. log τ plots (where τ = time between potential steps) were dependent on the chemical reactions associated with the electrochemical step. In particular, for an electrochemical step followed by a disproportionation there was considerable variation in the position of the I vs. log τ curves, whereas for an ECE process (for example), the curves were essentially invariant with applied potential. In the present case, such studies revealed very considerable variation of the curves with applied potential, which we interpret to be more consistent with a scheme based on disproportionation rather than a free-radical process.

Flash Photolysis Studies. The technique of flash photolysis can be used for observing photochemically generated transients and for measuring their rates of reaction.[31] For example, the strongly luminescent charge-transfer excited state of $Ru(bpy)_3^{2+}$ has received considerable attention: $Ru(bpy)_3^{2+*}$ undergoes rapid quenching by a bimolecular electron-transfer process, and flash photolysis methods have been used to rapidly generate $Ru(bpy)_3^{3+}$ and to study its subsequent reactions, particularly electron transfer.[32]

The technique of flash photolysis is particularly appropriate for studies of the present system, as it allows variation of $[H^+]$ (which was not possible for the chemical oxidation studies) and [Ru(III)] (by variation of the flash intensity). This appears to be the first use of such methods for the detailed kinetic study of ligand oxidation reactions.

A solution of $Ru(bpy)_2ampy^{2+}$ in 1 M $HClO_4$ shows an emission spectrum with λ_{max} = 625 nm (excitation wavelength 471 nm). Laser photolysis studies indicate that the luminescence lifetime in the same medium is 192 ± 2 ns, and quenching studies in the presence of $Fe(OH_2)_6^{3+}$ showed the rate constant for quenching to be $(2.8 \pm 0.1) \times 10^9$ M^{-1} s^{-1}. Consequently, under the conditions used for conventional flash photolysis studies, a solution of $Ru(bpy)_2ampy^{2+}$ containing the appropriate proportion of $Fe(OH_2)_6^{3+}$ can be used to generate $Ru(bpy)_2ampy^{3+}$ very rapidly;

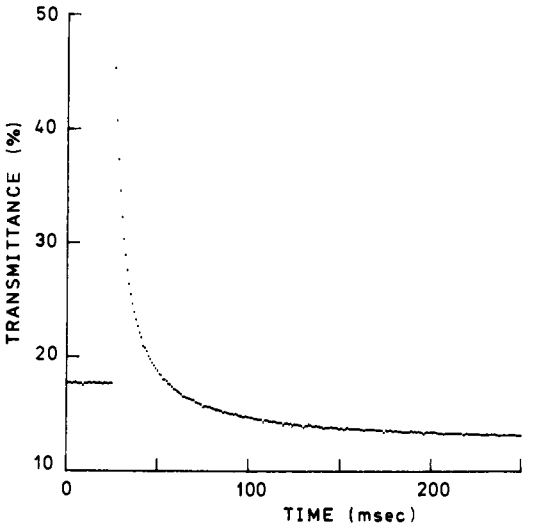

Figure 5. Typical transmittance–time response (followed at λ = 436 nm) from flash photolysis study of oxidation of $Ru(bpy)_2ampy^{2+}$ ($[HClO_4]$ = 1.0 M; T = 24.0 ± 0.5 °C).

in fact, in the lifetime of the flash used (<10 μs).

Studies were undertaken in aqueous perchloric acid media (0.01–1.00 M) by using a complex concentration of 1.01×10^{-5} M and quencher concentration $[Fe(OH_2)_6^{3+}]$ = 0.002 M. Perchlorate media were used in preference to sulfate to facilitate control of ionic strength over the range of acid concentrations used. The flash intensity was also systematically varied for a chosen set of conditions to change the [Ru(III)] produced during the flash. Conversions from Ru(II) → Ru(III) of ca. 30% were obtained, and a typical response curve is shown in Figure 5.

The responses were tested against the mechanistic schemes proposed earlier in the same manner as the chemical oxidation data. It was found that the results were entirely consistent with the scheme shown in eq 6–9, and as for the chemical oxidation data two solutions were found in the minimization procedure. The values of the rate constants and extinction coefficient for each numerical solution in both $HClO_4$ media and 1 M H_2SO_4 are given in Table I.

Calculated Rate Constants. The mechanistic scheme proposed is somewhat different to the kinetically analogous path in which the Ru(III) species formed by reaction 6 would disproportionate as shown in eq 10, with subsequent deprotonation to give the

$$2(bpy)_2Ru^{III}ampy^{3+} \underset{k_b}{\overset{k_f}{\rightleftharpoons}} (bpy)_2Ru^{II}ampy^{2+} + (bpy)_2Ru^{IV}ampy^{4+} \quad (10)$$

Ru^{IV}(ampy-H) species. This alternative scheme is identical with that proposed by Tovrog et al.[14] for the ruthenium-promoted oxidation of a coordinated alcohol. However, in both this case and that reported by Tovrog et al.,[14] the disproportionation process (k_f/k_b) would seem thermodynamically prohibited. For the system $Ru(bpy)_2Cl_2$, the $E_{1/2}$ for the Ru(III)/Ru(II) couple is 0.32 V vs. SSCE (acetonitrile solution; platinum bead electrode), whereas the corresponding Ru(IV)/Ru(III) couple occurs at 1.98 V.[33] It is a reasonable assertion that for the $Ru(bpy)_2ampy^{n+}$ system, the difference in potential between the Ru(IV)/Ru(III) and Ru(III)/Ru(II) couples is >1.0 V, so that for the disproportionation reaction (10), $K < 10^{-17}$: consequently, the formation of the Ru(IV) species by this means is unlikely. However, if the Ru(III) species were to deprotonate, the alternative path shown in eq 8 for the formation of a Ru(IV) intermediate is available.

The Ru(IV)/Ru(III) couple for the deprotonated amine species would be expected to be considerably cathodic of the couple for the nondeprotonated species. Such a reduction in potential is

(29) Hanafey, M. K.; Scott, R. L.; Ridgeway, T. H.; Reilly, C. N. *Anal. Chem.* **1978**, *50*, 116–137.
(30) Marcoux, L. *J. Phys. Chem.* **1972**, *76*, 3254–3259.
(31) Bock, C. R.; van Gustorf, E. A. K. *Adv. Photochem.* **1977**, *10*, 221–309.
(32) Bock, C. R.; Meyer, T. J.; Whitten, D. G. *J. Am. Chem. Soc.* **1974**, *96*, 4710–4712.
(33) Weaver, T. R.; Adeyemi, S. A.; Brown, G. M.; Eckberg, R. P.; Hatfield, W. E.; Johnson, E. C.; Murray, R. W.; Untereker, D.; Meyer, T. J. *J. Am. Chem. Soc.* **1975**, *97*, 3039–3048.

Table II. Rate Constants for the Scheme Given in Eq 6-9 Using Rate Data from Flash Photolysis in Perchlorate Media (λ = 436 nm; μ = 1.0, $NaClO_4$; T = 24 ± 1 °C; All Solutions Deaerated)

[H⁺], M	$10^{-6}k_2$, s^{-1}	$10^{-9}k_3$, M^{-1} s^{-1}	$10^{-9}k_4$, M^{-1} s^{-1}	$10^{-6}k_5$, M^{-1} s^{-1}	k_6, s^{-1}	ϵ, M^{-1} cm^{-1}
0.01[a]	5.1	1.4	9.0	5.1	94	1250[d]
0.01[a]	5.3	1.6	1.1	5.3	90	1250[d]
0.1	4.9	1.2	1.3	5.6	93	1250[d]
1.0[b]	5.0	1.4	1.0	5.4	92	1250
1.0[b]	5.2	1.2	1.1	5.3	93	1250
1.0[b]	5.1	1.3	1.0	5.3	93	1250
1.0[b]	5.2	1.3	1.1	5.4	94	1250
average values[c]	5.1 (±0.2)	1.3 (±0.2)	1.1 (±0.2)	5.3 (±0.2)	93 (±3)	1250

[a] Duplicate determinations. [b] These determinations were made by using different flash intensities but with all other conditions constant. [c] Errors quoted are experimental deviations. [d] ϵ set for optimum obtained from studies in 1 M $HClO_4$.

observed generally on lowering of overall complex charge[34] as, for example, in a Pt(IV) complex of a "cage" nitrogen macrocycle where a single deprotonation has been observed to stabilize the Pt(IV) state by 1.1 V.[35] Consequently, for the two couples involved in the electron-exchange reaction (8) $(Ru(bpy)_2(ampy)^{3+/2+}$ and $Ru(bpy)_2(ampy\text{-}H)^{3+/2+}$) the difference in potentials may be anticipated to be considerably less than 1 V, and possibly even negative, so that the equilibrium constant would be considerably more favorable which would allow formation of the deprotonated Ru(IV) species.

It should be noted that the stopped-flow data were obtained at 20 °C and the flash photolysis data at 24 °C, so that some care is needed in the comparison of results obtained from the two techniques. However, it is immediately clear that the results are comparable. The agreement between the calculated and experimental results is excellent for both numerical solutions, the sum of the squares of the absorbance differences between the generated curve and the data being less than 1×10^{-4} (50 points) for the flash photolysis experiments, and less than 3×10^{-4} (50 points) for the stopped-flow data.

For the stopped-flow method, six runs were taken under the same experimental conditions and the averaged run then used as data for the numerical analysis. The data obtained have limited accuracy since the observed transmittance change is relatively small, because the initial oxidation reaction (k_1) and subsequent ligand reactions are comparable in rate. All stopped-flow data were obtained in 1 M H_2SO_4 solution, as discussed earlier.

For each set of conditions using the flash photolysis technique, data were recorded in at least triplicate, and the individual runs were each analyzed. Runs were done in both sulfuric acid and perchloric acid media over the range [H⁺] = 0.01–1.00 M, and [Ru(III)] was varied by altering the intensity of the flash for solutions [H⁺] = 1.00 M. In Table I, the rate constants and extinction coefficient obtained for the two numerical solutions using data at 1 M H_2SO_4 are quoted for comparison with the stopped-flow results. The results given for perchloric acid media represent the average values obtained over the full range of conditions studied. In the following discussion, the rate constants and extinction coefficients quoted are those from the determinations in perchloric acid, since these correspond to the data of greatest precision.

***k*₁.** The value of k_1 for the oxidation of $Ru(bpy)_2ampy^{2+}$ by Ce(IV) in 1 M H_2SO_4 was found to be $(5.0 \pm 1.0) \times 10^5$ M^{-1} s^{-1}: this is in good agreement with the rate constant for the oxidation of $Ru(tpy)(bpy)NH_3^{2+}$ under the same conditions (k = $(6.1 \pm 0.2) \times 10^5$ M^{-1} s^{-1}). Since the $E_{1/2}$ values for the Ru^{III}/Ru^{II} couples in $Ru(tpy)(bpy)NH_3^{n+}$ and $Ru(bpy)_2ampy^{n+}$ are respectively 1.02 and 1.12 V vs. SSCE in acetonitrile, it would be expected that the rate of the oxidation of $Ru(bpy)_2ampy^{2+}$ was slightly slower than that of $Ru(tpy)(bpy)NH_3^{2+}$.

***k*₂, *k*₃.** For the two solutions of the numerical analysis, the values for $k_2 = 5 \times 10^6$ or 5×10^9 s^{-1} and the corresponding $k_3 = 1 \times 10^9$ or 1×10^{10} M^{-1} s^{-1}. Accordingly, the pK_a value would be either 2.4 or 0.3. The diffusion-controlled limits for the protonation of amines by the hydronium ion have been found to be in the range 10^9–10^{11} M^{-1} s^{-1},[36,37] and both solutions for k_3 are within this range. However, for the reprotonation of an analogous conjugate base complex, $[Pt(en)_2(en\text{-}H)]^{3+}$, the rate is 1.9×10^9 M^{-1} s^{-1} (at 27 °C):[36] this is consistent with $k_3 = 1.3 \times 10^9$ M^{-1} s^{-1} for numerical solution (i) (Table I) in the present system. On this basis, we are inclined to prefer solution (i) to explain the experimental observations, and a detailed summary of the results of the numerical solution (i) for the minimization procedure using data from flash photolysis experiments in perchlorate media is given in Table II.

The pK_a value for the equilibrium given in eq 7 of the scheme is therefore 2.4. For $Ru(NH_3)_6^{3+}$, the pK_a = 13.1[38] and the ammine protons are significantly more acidic for $Ru(NH_3)_5py^{3+}$ ($pK_a \approx 9$)[23], presumably because the presence of the pyridine ligand increases the Lewis acidity of the Ru(III) center. For the corresponding $Ru(bpy)_2ampy^{3+}$ complex with five pyridine-type ligands, the pK_a of the amine protons would be expected to be significantly lower, so that 2.4 would seem a reasonable value. The fact that the $-NH_2$ group is part of a chelate ring may also contribute to a lowering of the pK_a, as models of the ring system indicate that there is some strain present.

***k*₄, *k*₅.** The forward rate constant (k_4) for the disproportionation in the scheme may be estimated from electron-transfer studies of similar ruthenium complexes. The disproportionation step is an electron transfer between two $Ru^{III}(bpy)_2ampy$ molecules, one of which is deprotonated. The electron-transfer rate between tris(bipyridine)ruthenium(II) and tris(1,10-phenanthroline)ruthenium(III) is 2×10^9 M^{-1} s^{-1},[39] so that the value obtained of 1×10^9 M^{-1} s^{-1} for k_4 is not unreasonable. The equilibrium constant for reaction 8 ($K \approx 208$) implies that there is a difference of ~0.14 V between the potentials of the two couples involved in the equilibrium. Since in H_2SO_4 media, $E_{1/2} \approx 0.7$ V for the $Ru(bpy)_2ampy^{3+/2+}$ couple, it can be calculated that $E_{1/2} \approx 0.56$ V for the Ru(IV)/Ru(III) couple for the deprotonated species, which is in the range expected (vide supra).

***k*₆.** The rate constant obtained is constant on varying both acid and Ru(III) concentrations (93 s^{-1}). However, although this process has been written as a single step, it clearly involves transfer of two electrons from the ligand to the metal, together with a single deprotonation from the methylene carbon group. It is unlikely these acts would be simultaneous and it is unclear as to whether the electron transfer would involve a concerted two-electron process or two consecutive one-electron steps. To satisfy the observed kinetics, one of these processes, or the deprotonation, or a concerted process would be rate determining with any remaining steps being rapid.

ϵ. The values of the molar extinction coefficient for the $(bpy)_2Ru^{IV}$ complex of deprotonated 2-(aminomethyl)pyridine were ϵ_{471} = 300 M^{-1} cm^{-1} (determined from stopped-flow measurements) and ϵ_{436} = 1250 M^{-1} cm^{-1} (determined from flash

(34) Brown, G. M. Ph.D. Thesis, University of North Carolina at Chapel Hill, 1974.
(35) Lawrance, G. A.; Lay, P. A.; Sargeson, A. M., unpublished work.
(36) Eigen, M. *Angew., Chem. Int. Ed. Engl.* **1974**, *3*, 1–19.
(37) Pitner, T. P.; Martin, R. B. *J. Am. Chem. Soc.* **1971**, *93*, 4400–4405.
(38) Waysbort, D.; Navon, G. *Inorg. Chem.* **1979**, *8*, 9–13.
(39) Young, R. C.; Keene, F. R.; Meyer, T. J. *J. Am. Chem. Soc.* **1977**, *99*, 2468–2473.

photolysis measurements). These values correspond to values obtained for the analogous Ru(IV) complex $[(tpy)(bpy)Ru^{IV}=O]^{2+}$ [28] for which $\epsilon_{471} = 550\ M^{-1}\ cm^{-1}$ and $\epsilon_{436} = 1150\ M^{-1}\ cm^{-1}$.

It seems, therefore, that the values of the rate constants are consistent with comparable electron-exchange and proton-transfer processes, and that the extinction coefficients of the proposed intermediate are consistent with those of a comparable Ru(IV) species. It should be stressed that the curve-fitting procedure produced two numerical solutions, one of which appears to be marginally more satisfactory. The consistency in the values of all variables, and particularly of k_6 on variation of both acid and Ru(III) concentration, leads us to have considerable confidence in the method. The method is quite sensitive to changes in the quoted values of the rate constants: in particular, for the fit to be maintained between the calculated and observed responses, the values of k_1, k_6, ϵ, and the ratio k_2/k_3 are critical and are required to be within 10% of the values quoted. The rate constants k_4 and k_5 are less critical (±25%). Although the ratio k_2/k_3 must be within 10%, the actual values of the individual rate constants, k_2 and k_3, may vary by a factor of 2.

Conclusions

The particular efficacy of Ru in the promotion of the oxidative dehydrogenation of an amine such as 2-(aminomethyl)pyridine seems related to its ability to readily attain an oxidation state 2 units greater than the final state, allowing a low-energy pathway for the even-electron process required in these dehydrogenation reactions. We are presently extending these methods of flash photolysis and electrochemistry to other oxidative dehydrogenation reactions to examine the generality of the scheme for ruthenium complexes containing other amines and alcohols and to assign unambigously the mechanistic schemes for such reactions involving alternative metal centers.

Acknowledgment. We wish to acknowledge the Australian Institute of Nuclear Science and Engineering for the use of stopped-flow facilities of the Australian Atomic Energy Commission, Lucas Heights. We are grateful to the Department of Physical and Inorganic Chemistry, University of Adelaide, for the use of the flash photolysis facilities, and particularly to Dr. G. S. Laurence and Ms. P. Ashwood for their assistance. We thank the Australian Research Grants Committee for supporting this research.

Appendix

Analysis of Experimental Data. In view of the complexity of the reaction mechanisms proposed in the study, analytical solution of the rate law equations was not possible: a numerical technique was required in order to analyze the experimental responses.

The numerical problem is to solve systems (up to 7) of coupled differential equations which define the rate laws. Due to the large possible variation in the magnitude of the rate constants within the proposed mechanism, the coupled differential equations are "stiff",[40] and conventional numerical differential equation algorithms such as the Runge-Kutta algorithm cannot efficiently be used. Algorithms have been specifically designed for the solution of stiff sets of equations of which the method of Gear, used in this study, is in most common use (IMSL library routine DGEAR[41]).

Kinetic information is available from the experimental responses by finding the set of rate constants for a given mechanism which minimize the sum of squares difference between the predicted and experimental response. Nonlinear programming (NLP) techniques automatically vary the rate constants such that this minimum is obtained rapidly. The two NLP techniques used were the simplex algorithm and a Marquadt Steepest Descent algorithm, the latter being the more efficient, but both were found to converge to the same solutions for certain problems, thus confirming the validity of the results.

The possibility of local rather than global optima having been reached was diminished by supplying largely varying initial values of the rate constants and observing convergence to the same optimal solution.

(40) Ebert, K. H.; Ederer, H. J.; Isbarn, G. *Angew. Chem., Int. Ed. Engl.* **1980**, *19*, 333-343.
(41) International Mathematical and Statistical Libraries, 1979, Vol. 7.

The Mechanism and Kinetics of the Homogeneous Gas-Phase Thermal Decomposition of Methylgermane

J. Dzarnoski, H. E. O'Neal,* and M. A. Ring*

Contribution from the Department of Chemistry, San Diego State University, San Diego, California 92182. *Received January 12, 1981*

Abstract: The homogeneous gas-phase decomposition of methylgermane has been investigated by the comparative rate-single-pulse shock tube technique at 3100 torr of total pressure between 1050 and 1250 K. Three primary processes occur: $CH_3GeH_3 \rightarrow CH_3GeH + H_2$ (1), $CH_3GeH_3 \rightarrow CH_4 + GeH_2$ (2), and $CH_3GeD_3 \rightarrow CH_2{=}GeD_2 + HD$ (3). The overall decomposition rate constant in its pressure falloff regime is $\log k_0\ (s^{-1}) = 13.34 - 50\,420 \pm 3700\ \text{cal}/\theta$, comprised of about 40% of reaction 1, and 30% each of reactions 2 and 3; and the high-pressure rate constants for the primary processes, obtained by RRKM calculations, are $\log k_1\ (s^{-1}) = 14.6 - 50\,400\ \text{cal}/\theta$, $\log k_2\ (s^{-1}) = 14.9 - 51\,600\ \text{cal}/\theta$, and $\log k_3\ (s^{-1}) = 14.7 - 51\,600\ \text{cal}/\theta$. The decomposition of the primary product methylgermylene (CH_3GeH) to $CH_3\cdot$ and GeH radicals increases with increasing temperature with an activation energy of about 53 kcal, while the decomposition of germylene (GeH_2) to Ge and H_2 is fast and complete at shock temperatures.

Comparisons of the decompositions of silicon and germanium compounds reveal some interesting similarities and also some interesting differences. For instance, both silane (SiH_4) and germane (GeH_4) decompose by a three-center hydrogen elimination process to produce singlet diradicals (silylene, SiH_2:, and germylene, GeH_2:).[1,2] However, under static system pyrolysis conditions ($T - 600$ K), the silane decomposition is homogeneous[3] (at least in the initial stages), while the germane decomposition appears to be mainly heterogeneous.[2] Both group 4 hydride decompositions have stoichiometries approaching $(\Delta(H_2)/\Delta-$

(1) C. G. Newman, H. E. O'Neal, M. A. Ring, F. Leska, and N. Shipley, *Int. J. Chem. Kinet.*, **11**, 1167 (1979).
(2) C. G. Newman, J. Dzarnoski, M. A. Ring, and H. E. O'Neal, *Int. J. Chem. Kinet.*, **12**, 661 (1980).
(3) J. H. Purnell and R. Walsh, *Proc. R. Soc. London, Ser. A*, **293**, 543 (1966).

0002-7863/81/1503-5740$01.25/0 © 1981 American Chemical Society